Synthesis and Characterization of Single-Crystal Strontium Hexaboride Nanowires

ARTICLE *in* NANO LETTERS · NOVEMBER 2008

Impact Factor: 13.59 · DOI: 10.1021/nl8021225 · Source: PubMed

NANO LETTERS

Letter

Synthesis and Characterization of Single-Crystal Strontium Hexaboride Nanowires

Panchatapa Jash, Alan W. Nicholls, Rodney S. Ruoff, and Michael Trenary

Nano Lett., **2008**, 8 (11), 3794-3798 • DOI: 10.1021/nl8021225 • Publication Date (Web): 25 October 2008

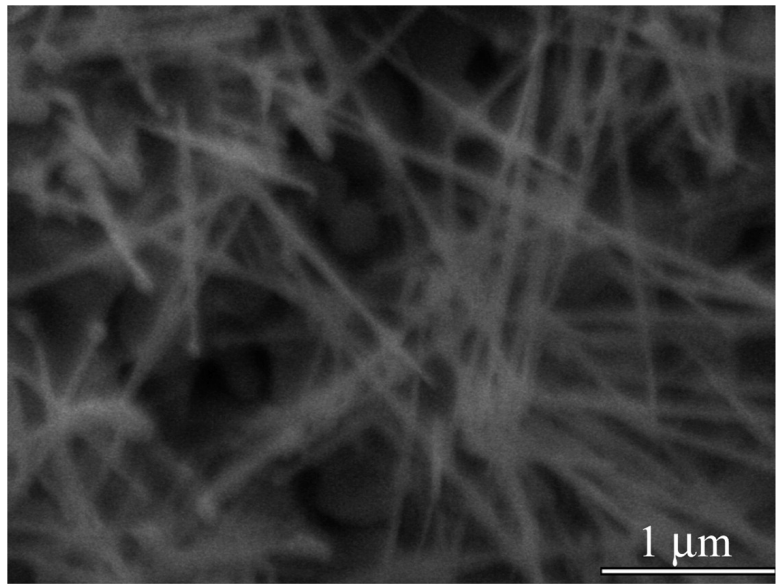

More About This Article

Additional resources and features associated with this article are available within the HTML version:

- Supporting Information
- Access to high resolution figures
- Links to articles and content related to this article
- Copyright permission to reproduce figures and/or text from this article

View the Full Text HTML

NANO LETTERS

2008
Vol. 8, No. 11
3794-3798

Synthesis and Characterization of Single-Crystal Strontium Hexaboride Nanowires

Panchatapa Jash,[†] Alan W. Nicholls,[‡] Rodney S. Ruoff,[§] and Michael Trenary*[,†]

Department of Chemistry and Research Resources Center, University of Illinois at Chicago, Chicago, Illinois, 60607, and Department of Mechanical Engineering, University of Texas, Austin, Texas 78712

Received July 16, 2008; Revised Manuscript Received September 20, 2008

ABSTRACT

Catalyst-assisted growth of single-crystal strontium hexaboride (SrB_6) nanowires was achieved by pyrolysis of diborane (B_2H_6) over SrO powders at 760−800 °C and 400 mTorr in a quartz tube furnace. Raman spectra demonstrate that the nanowires are SrB_6, and transmission electron microscopy along with selected area diffraction indicate that the nanowires consist of single crystals with a preferred [001] growth direction. Electron energy loss data combined with the TEM images indicate that the nanowires consist of crystalline SrB_6 cores with a thin (1 to 2 nm) amorphous oxide shell. The nanowires have diameters of 10−50 nm and lengths of 1−10 μm.

There have been many reports in the recent literature on the growth of nanocrystalline forms of metal hexaborides.[1−8] These studies have been motivated by the general idea that nanostructured forms of materials will display enhanced properties beyond those of the bulk forms of the same materials. Hexaborides of the general formula MB_6, where M is a rare earth or alkaline earth metal, are generally extremely hard, refractory solids with high chemical stabilities.[9−11] From the earliest considerations of the electronic structure of metal hexaborides,[12] it was predicted that those formed from trivalent metals would be metallic electrical conductors, whereas the hexaborides of the divalent metals, such as Ca, Sr, Ba, and Eu, would be semiconductors. However, both theoretical and experimental studies of their electronic structures indicate that the hexaborides of divalent metals are difficult to classify. Much effort has focused on whether the materials have a finite band gap. Two recent independent electronic structure calculations indicate that CaB_6 is a semiconductor with an X-point band gap of 0.8 eV.[13,14] One angle-resolved photoemission spectroscopy (ARPES) study of CaB_6 confirmed an X-point band gap of 1 eV,[15] whereas another study using both ARPES and *k*-resolved resonant inelastic X-ray scattering indicated an X-point band gap of >1 eV with similar properties for SrB_6 and EuB_6.[16] An experimental study of a structurally well-characterized single crystal of SrB_6 showed that its electronic transport properties at both zero and nonzero frequencies above liquid ^{4}He temperatures are close to those of a semiconductor, whereas at very low temperatures, the compound enters a metallic state with a low concentration of itinerant charge carriers.[17] In general, whereas the extensive literature on hexaborides of divalent metals indicates that they have novel bulk properties, little is known about nanostructured forms of these materials. The work reported here on the synthesis and structural characterization of SrB_6 nanowires constitutes the necessary first step for further exploration of the properties of nanoscale forms of this material.

Although it is of general interest to prepare nanowire forms of materials with interesting bulk properties, a specific motivation for establishing methods for the synthesis of nanowires of alkaline earth hexaborides and other boron-rich solids is for their potential application as thermoelectric materials.[18−20] The overall efficiency of a thermoelectric material is given by the dimensionless parameter $ZT = \alpha^2\sigma T/\kappa$, where α is the Seebeck coefficient, σ is the electrical conductivity, κ is the thermal conductivity, and T is the absolute temperature. A recent study[21] of the thermoelectric properties of the bulk hexaborides of Ca, Sr, and Ba showed that these materials have very favorable Seebeck coefficients and electrical conductivities, which makes them potentially attractive for high-temperature thermoelectric applications. Of the three, SrB_6 had the highest power factor, but its ZT value was still low because of its rather high thermal conductivity compared with other thermoelectric materials. Takeda et al.[21] sought to decrease the thermal conductivity

* Corresponding author. Tel: (312) 996-0777. Fax: (312) 996-0431. E-mail: mtrenary@uic.edu.
[†] Department of Chemistry, University of Illinois at Chicago.
[‡] Research Resources Center, University of Illinois at Chicago.
[§] University of Texas at Austin.

10.1021/nl8021225 CCC: $40.75
Published on Web 10/25/2008

of SrB_6 by adding Ca to form bulk $Sr_xCa_{1-x}B_6$ alloys. However, a promising new strategy for decreasing κ without necessarily decreasing α and σ is to prepare thermoelectric materials in nanowire and other low dimensional forms.[22] For this reason, the development of methods for the synthesis of SrB_6 nanowires should be of specific interest to the field of thermoelectric materials, which in turn is of current general interest as a way to use and generate energy more efficiently.[23]

A second unrelated motivation for establishing methods of preparing alkaline earth hexaborides in nanocrystalline form stems from a recent report showing that CaB_6 is one of the products in the reversible dehydrogenation of $Ca(BH_4)_2$, and the latter compound is therefore of great interest as a potential hydrogen storage material.[24] The kinetics of the reaction of CaB_6 with hydrogen to form $Ca(BH_4)_2$ is likely to be enhanced if the hexaboride is in nanocrystalline form, as was recently shown for sodium alanate,[25] another potential hydrogen storage material.

The present work on SrB_6 uses the same methodology as that described in an earlier study on the synthesis of CaB_6 nanowires.[1] In a more recent report,[26] CaB_6 nanowires were grown by a self-catalyzed method using Ca metal and BCl_3 gas in a simple CVD reactor. This method was promoted as a way to avoid the use of the hazardous diborane precursor, although BCl_3 also requires careful handling. More significantly, the BCl_3 method produced wires with diameters of $\sim$100 nm, whereas CaB_6 nanowires with diameters as small as 15 nm were reported by Xu et al.[1] Because nanowires with the smallest diameters are of most interest, we have followed the procedures of ref 1.

The nanowires were grown in a low-pressure chemical vapor deposition (LPCVD) apparatus that was constructed following a design described in detail in a study where it was used for the growth of boron nanoribbons.[27] The SrB_6 was deposited on silicon (Si) substrates (University Wafer) covered with 1-μm-thick thermally grown SiO_2 films. The substrates were ultrasonically cleaned by the use of a 1:2 H_2O_2/H_2SO_4 solution, followed by acetone and ethanol (ultrasonic cleaner, 5 min). SrO powders (Alfa Aesar, 99.9% purity) were randomly deposited on the Si substrates. A thin Ni layer (5 to 6 nm) was then evaporated on the SrO-coated Si substrate by a low-pressure thermal evaporator. The substrates were loaded in a quartz boat and placed in a 1 in. diameter quartz tube reaction chamber. The chamber temperature was ramped up to 925 °C (center position temperature) in 45 min with a 5 sccm (standard cubic centimeters per minute) continuous flow of argon (Air Gas, 99.999% purity). A gas mixture of diborane (Matheson TriGas, 1.08% UHP diborane in research grade argon, flow rate: 20 sccm) was then introduced to the chamber for 75 min. The reaction pressure for each run was 400 mTorr. After the reaction, the chamber was cooled to room temperature in 5 h under 5 sccm argon flow. Gray deposits were visible to the naked eye and were further characterized with the techniques of Raman spectroscopy (Renishaw Ramascope-2000, 514.5 nm argon ion laser excitation, spectral resolution of 2 cm^{-1} and spatial resolution of 1 μm), scanning electron microscopy (SEM, JEOL JEM-6320F), and transmission electron microscopy (TEM, JEOL JEM-2010F) including selected area electron diffraction (SAED) and electron energy loss spectroscopy (EELS).

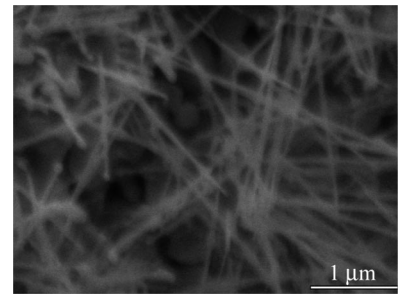

Figure 1. SEM micrograph of the SrB_6 nanowires.

Figure 1 is an SEM image of the as-synthesized nanowires. The nanowires are straight and have uniform diameters between 10 and 40 nm with lengths of several micrometers. Although not readily apparent from the image in Figure 1, most of the nanowires have bulbous tips that are likely due to Ni catalyst particles, as was observed for CaB_6 nanowires.[1]

The SEM images in Figure 2, with lower magnification images as insets, show three different nanowire morphologies obtained at three different temperatures. The wires shown in Figure 2a were grown in a relatively low-temperature region of the furnace ($\sim$700 °C) and are thicker ($\sim$50−60 nm) and shorter ($\sim$1 μm in length) than those grown in the higher temperature (between 750 and 800 °C) regions used for the growth of the wires shown in Figure 2b,c, which have diameters between 10 and 40 nm and are several micrometers long. These wires have either uniform diameters (Figure 2b or at the center of Figure 2c) or a tapered structure (lower left corner of Figure 2c).

Figure 3 shows a Raman spectrum acquired at room temperature and ambient pressure of the same nanowires used for the SEM image of Figure 1. The expected Raman active modes for B_6 octahedra (O_h point group) are the F_{2g} bending and E_g and A_{1g} stretching modes. For SrB_6, the F_{2g}, E_g, and A_{1g} fundamentals appear at 765, 1075, and 1222 cm^{-1}, respectively. Table 1 compares the peak positions observed for our nanowires with literature values for SrB_6 in powder form.[28,29] The comparison proves that the nanowires are composed of SrB_6. The shoulders and weaker features reported for the SrB_6 powders are not apparent in our spectra. This difference is not due to broadening of the nanowire peaks because the fwhm of the ν_4 (F_{2g}), ν_2 (E_g), and ν_1 (A_{1g}) fundamentals are 24, 35, and 47 cm^{-1}, respectively, and are comparable to those of the powdered sample.[29] The difference is likely due to defects or impurities present in the powder that are absent in the nanowires.

Although EELS spectra are often used to quantify the elemental composition of a material, this is not possible in this case because the boron K-shell edge (188 eV) overlaps with the strontium $M_{4,5}$-shell edge (133 eV). We therefore measured and compared EELS spectra of a SrB_6 nanowire and of commercially available SrB_6 powder (Aldrich, 99%, 325 mesh = 44 μm particle size), as shown in Figure 4. The

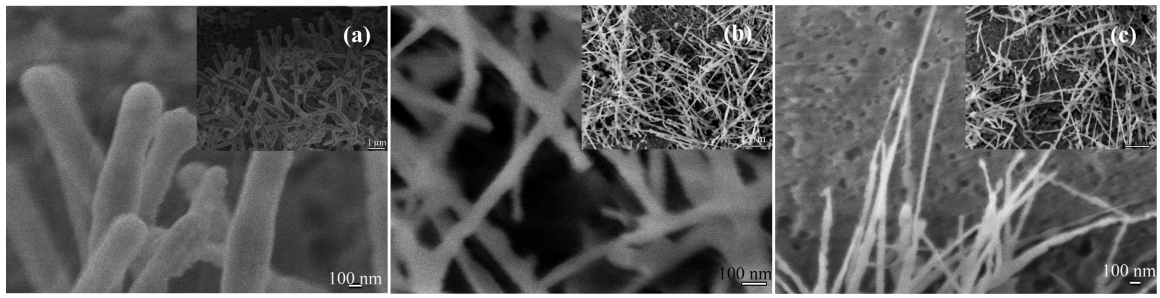

Figure 2. SEM images of different SrB6 nanowire morphologies corresponding to regions of the furnace at (a) 700, (b) 750, and (c) 800 °C.

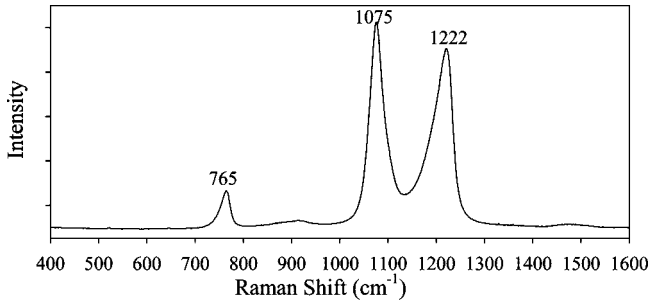

Figure 3. Raman spectrum of the SrB_6 nanowires collected from the same sample used for the SEM micrograph of Figure 1.

Table 1. Summary of Raman Peak Positions of SrB_6

	peak position (cm^{-1})		
materials	A_{1g}	E_g	F_{2g}
calculated[28]	1270	1141	775
SrB_6 powders[28]	1258	1160w	770m
		1122m	752sh
SrB_6 powders[29]	1225s	1192sh	760s
		1105sh	732sh
		1078s	
SrB_6 nanowires[a]	1222	1075	765

[a] Measured in this work.

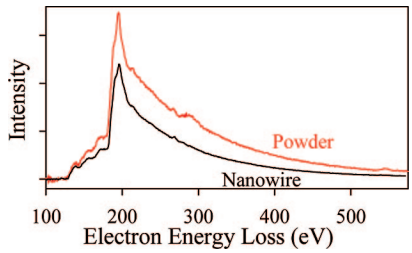

Figure 4. Comparison of EELS spectra of a SrB_6 nanowire with EELS spectra of commercially available SrB_6 powder.

spectra, which have been background corrected, clearly indicate that the edge height ratio of Sr to B in the two samples is the same. The small peak at 283 eV for SrB_6 powder is from the carbon support film.

The EELS line scans (STEM mode; probe size 0.2 nm) shown in Figure 5 provide information on the elemental distribution across the nanowires and were recorded without background subtraction from the center and edges of one nanowire. The edge spectra show the characteristic B and O ionization edges at 188 and 532 eV, respectively. However, the O K-shell ionization edge is not seen in the spectrum obtained at the center of the nanowire, indicating that an

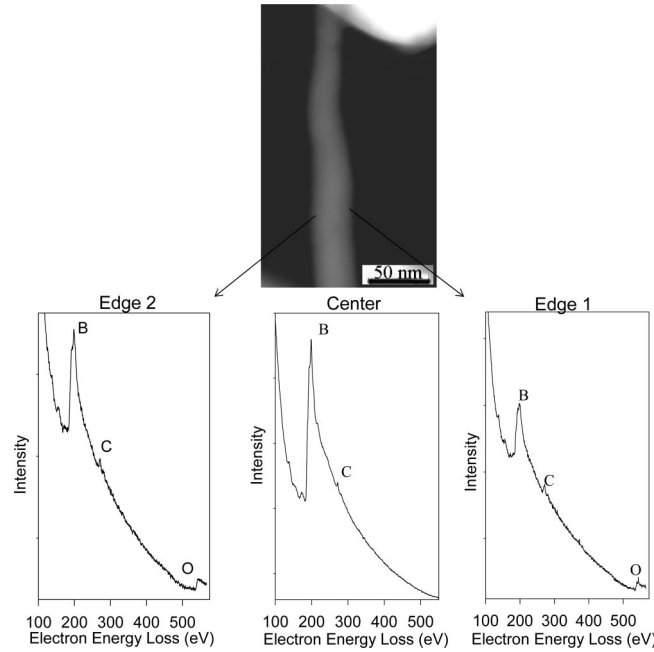

Figure 5. EELS spectra from the edges and center of a SrB_6 nanowire showing that oxygen is present at only the edges.

oxide layer forms a thin shell around a pure SrB_6 center.

Most hexaborides, whether formed by divalent or trivalent metals, have the simple CaB_6 structure (space group $Pm3m$-O_h^1) with the metal atom at the center of a cube and B_6 octahedra at the eight cube corners, as originally reported.[30−32] The structure can also be described as two interpenetrating simple cubic lattices with metal atoms occupying the sites of one sublattice and B_6 octahedra occupying the sites of the second sublattice. The B_6 octahedra are covalently bonded to B_6 octahedra of adjacent unit cells to form a rigid 3D covalently bonded boron lattice. Because the boron lattices largely determine the lattice constants, they show little variation among the hexaborides; for example, those of CaB_6 and LaB_6 have almost identical values of 4.146 and 4.154 Å, respectively, and that of SrB_6 is only slightly larger at 4.198 Å.[11]

Structural characterization of the SrB_6 nanowires along three different zone axes with the high-resolution TEM images and the selected-area diffraction patterns of Figure 6 are indicative of high crystalline quality with a low density of defects. Only reflections corresponding to the SrB_6 structure were observed in the diffraction patterns. No diffuse

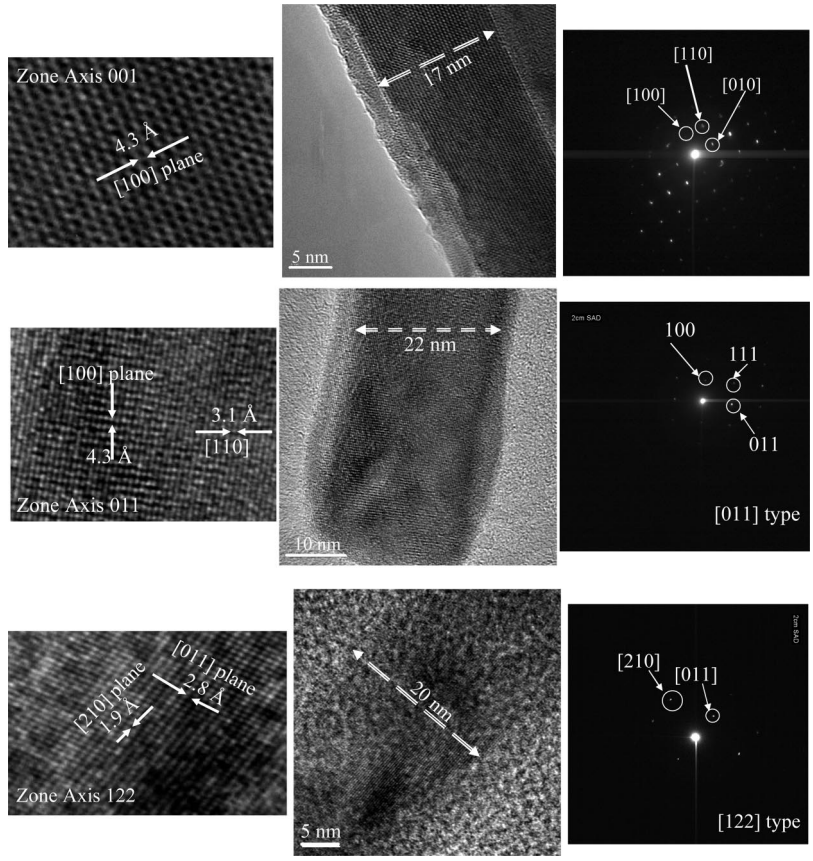

Figure 6. High-resolution TEM images (left two panels) and SAED patterns (right) along the [001] (top), [011] (middle), and [112] (bottom) zone axes of the SrB_6 nanowires.

scattering or superstructure reflections were detected. The TEM images show that the nanowires consist of a central crystalline core with a 1-to-2-nm-thick amorphous shell. The presence of oxygen at the edges of a nanowire, as revealed by the EELS results shown in Figure 5, implies that the amorphous shell seen in the TEM images consists of an oxide. Further compositional information was obtained from EDX spectra collected from the same wires as those from which the TEM images of Figure 6 were obtained but did not show the presence of Ni, indicating that its concentration must be less than 0.1 atomic percent. Although Ni would be expected to be present in the Ni catalyst particles seen with SEM, these particles were not observed with TEM, in contrast with what was observed by Xu et al.,[1] where all of their CaB_6 nanowires were terminated with Ni catalyst particles. It may be that the Ni particles were detached during the TEM sample preparation, in which an ultrasonic bath was used to form a suspension of the nanowires in isopropyl alcohol. Because this procedure also resulted in breaking the wires into shorter lengths, it is also likely that the Ni particles became detached. It is also possible that the Ni particles were consumed at the end of the growth process.

In their report on CaB_6 nanowires, Xu et al.[1] concluded that growth occurred by the Ni-catalyzed vapor−liquid−solid (VLS) mechanism in which small miscible Ca−B−Ni liquid alloy droplets acted as nucleation sites.[33] The following two observations suggest that the SrB_6 nanowires described here grew by the same mechanism: First, Ni catalyst particles were observed at the tip of some of the nanowires, and second, the reaction temperature (700−800 °C) was lower than most reported values for the synthesis of SrB_6 powders (>1000 °C). This mechanism would involve the dissolution of Sr- and B-containing gas phase species in the Sr−B−Ni droplet. Because it provided the first synthetic route to higher boranes, the pyrolysis of gas phase B_2H_6 was extensively studied in the early days of borane chemistry, and the work through 1964 was reviewed by Adams.[34] In general, these studies involved temperatures much lower than those used here. For example, a plot of the species detected by vapor−liquid chromatography in the pyrolysis of B_2H_6 at 111 °C as a function of time shows B_4H_{10}, B_5H_{11}, and B_5H_9, with the latter species steadily increasing as the B_2H_6 concentration decreased.[35] The mechanism of decomposition was widely studied, and a variety of intermediates, including borane (BH_3), were postulated. Although it has long been known that at 700 °C diborane will completely decompose to deposit amorphous boron on the reactor walls, it is also possible that various boron hydrides are present as transient species and are responsible for transporting boron to the growing nanowire. The vaporization of SrO in vacuum generates a range of gaseous species, including Sr(g), O_2(g), O(g), and SrO(g),[36,37] whereas SrO evaporation in the presence of H_2(g) would presumably additionally generate SrOH(g) and $Sr(OH)_2$(g) by analogy to what is produced from CaO evaporation in H_2(g).[38] According to Asano et al.,[39] the partial pressure of Sr(g) is at least an order of magnitude higher

than that of SrO(g) above heated SrO(s), and extrapolating their results to our reaction temperature of roughly 1000 K yields a Sr(g) vapor pressure of 1.5×10^{-16} Torr.

In summary, crystalline SrB_6 nanowires were synthesized using LPCVD. The synthesis mechanism probably followed a Ni-catalyzed VLS pathway. Nanowires are 10−50 nm in diameter, depending on the synthesis temperature, and are about a micrometer to several micrometers in length, again depending on synthesis temperature. The Raman spectrum is in good agreement with previously published Raman spectra of SrB_6 powder. The nanowires consist of a crystalline SrB_6 core surrounded by a thin 1 to 2 nm amorphous oxide shell. Electron diffraction patterns along different zone axes show that the growth is mainly in the [001] direction.

Acknowledgment. This work was supported by a grant from the U.S. Department of Energy (grant no. DE-FG02-05ER15726).

References

(1) Xu, T. T.; Zheng, J. G.; Nicholls, A. W.; Stankovich, S.; Piner, R. D.; Ruoff, R. S. *Nano Lett.* **2004**, *4*, 2051.
(2) Ding, Q. W.; Zhao, Y. M.; Xu, J. Q.; Zou, C. Y. *Solid State Commun.* **2007**, *141*, 53.
(3) Brewer, J. R.; Deo, N.; Wang, Y. M.; Cheung, C. L. *Chem. Mater.* **2007**, *19*, 6379.
(4) Zhang, H.; Zhang, Q.; Tang, J.; Qin, L. C. *J. Am. Chem. Soc.* **2005**, *127*, 8002.
(5) Zhang, H.; Zhang, Q.; Zhao, G.; Tang, J.; Zhou, O.; Qin, L. C. *J. Am. Chem. Soc.* **2005**, *127*, 13120.
(6) Zhang, H.; Zhang, Q.; Tang, J.; Qin, L. C. *J. Am. Chem. Soc.* **2005**, *127*, 2862.
(7) Xu, J.; Chen, X.; Zhao, Y.; Zou, C.; Ding, Q.; Jian, J. *J. Cryst. Growth* **2007**, *303*, 466.
(8) Zou, C. Y.; Zhao, Y. M.; Xu, J. Q. *J. Cryst. Growth* **2006**, *291*, 112.
(9) Etourneau, J.; Mercurio, J.-P.; Hagemuller, P. In *Boron and Refractory Borides*; Matkovich, V. I., Ed.; Springer-Verlag: Berlin, 1977.
(10) Post, B. In *Boron, Metallo-Boron Compounds, and Boranes*; Adams, R. M., Ed.; Interscience Publishers: New York, 1964.
(11) Hoard, J. L.; Hughes, R. E. In *The Chemistry of Boron and Its Compounds*; Muetterties, E. L., Ed.; Wiley: New York, 1967; p 26.
(12) Longuet-Higgins, H. C.; Roberts, M. d. V. *Proc. R. Soc. London, Ser. A* **1954**, *224*, 336.
(13) Tromp, H. J.; van Gelderen, P.; Kelly, P. J.; Brocks, G.; Bobbert, P. A. *Phys. Rev. Lett.* **2001**, *87*, 016401.
(14) Wu, Z. G.; Singh, D. J.; Cohen, R. E. *Phys. Rev. B* **2004**, *69*, 193105.
(15) Souma, S.; Komatsu, H.; Takahashi, T.; Kaji, R.; Sasaki, T.; Yokoo, Y.; Akimitsu, J. *Phys. Rev. Lett.* **2003**, *90*, 027202.
(16) Denlinger, J. D.; Clack, J. A.; Allen, J. W.; Gweon, G. H.; Poirier, D. M.; Olson, C. G.; Sarrao, J. L.; Bianchi, A. D.; Fisk, Z. *Phys. Rev. Lett.* **2002**, *89*, 157601.
(17) Ott, H. R.; Chernikov, M.; Felder, E.; Degiorgi, L.; Moshopoulou, E. G.; Sarrao, J. L.; Fisk, Z. *Z. Phys. B: Condens. Matter* **1997**, *102*, 337.
(18) Werheit, H. *Mater. Sci. Eng., B* **1995**, *29*, 228.
(19) Imai, Y.; Mukaida, M.; Ueda, M.; Watanabe, A. *Intermetallics* **2001**, *9*, 721.
(20) Takeda, M.; Fukuda, T.; Domingo, F.; Miura, T. *J. Solid State Chem.* **2004**, *177*, 471.
(21) Takeda, M.; Terui, M.; Takahashi, N.; Ueda, N. *J. Solid State Chem.* **2006**, *179*, 2823.
(22) Dresselhaus, M. S.; Chen, G.; Tang, M. Y.; Yang, R. G.; Lee, H.; Wang, D. Z.; Ren, Z. F.; Fleurial, J. P.; Gogna, P. *Adv. Mater.* **2007**, *19*, 1043.
(23) Bell, L. E. *Science* **2008**, *321*, 1457.
(24) Ronnebro, E.; Majzoub, E. H. *J. Phys. Chem. B* **2007**, *111*, 12045.
(25) Baldé, C. P.; Hereijgers, B. P. C.; Bitter, J. H.; de Jong, K. P. *J. Am. Chem. Soc.* **2008**, *130*, 6761.
(26) Xu, J. Q.; Zhao, Y. M.; Zou, C. Y.; Ding, Q. W. *J. Solid State Chem.* **2007**, *180*, 2577.
(27) Xu, T. T.; Zheng, J. G.; Wu, N. Q.; Nicholls, A. W.; Roth, J. R.; Dikin, D. A.; Ruoff, R. S. *Nano Lett.* **2004**, *4*, 963.
(28) Yahia, Z.; Turrell, S.; Turrell, G.; Mercurio, J. P. *J. Mol. Struct.* **1990**, *224*, 303.
(29) Turrell, S.; Yahia, Z.; Huvenne, J. P.; Lacroix, B.; Turrell, G. *J. Mol. Struct.* **1988**, *174*, 455.
(30) Allard, G. *Bull. Soc. Chim.* **1932**, *51*, 1213.
(31) Pauling, L.; Weinbaum, S. *Z. Kristallogr.* **1934**, *87*, 181.
(32) von Stackelberg, M.; Neumann, F. *Z. Physik. Chem.* **1932**, *B19*, 314.
(33) Wagner, R. S.; Ellis, W. C. *Appl. Phys. Lett.* **1964**, *4*, 89.
(34) Adams, R. M. In *Boron, Metallo-Boron Compounds, and Boranes*; Adams, R. M., Ed.; Interscience Publishers: New York, 1964.
(35) Borer, K.; Littlewood, A. B.; Phillips, C. S. G. *J. Inorg. Nucl. Chem.* **1960**, *15*, 316.
(36) Samoilova, I. O.; Kazenas, E. K. *Rus. Metall.* **1994**, *3*, 36.
(37) *The Oxide Handbook*; Samsonov, G. V., Ed.; Plenum: New York, 1973.
(38) Farber, M.; Srivastava, R. D.; Moyer, J. W.; Leeper, J. D. *J. Chem. Soc., Faraday Trans.* **1987**, *83*, 3229.
(39) Asano, M.; Yamamoto, Y.; Sasaki, N.; Kubo, K. *Bull. Chem. Soc. Jpn.* **1972**, *45*, 82.

NL8021225